



ALMA MATER STUDIORUM  
UNIVERSITÀ DI BOLOGNA

## ARCHIVIO ISTITUZIONALE DELLA RICERCA

### Alma Mater Studiorum Università di Bologna Archivio istituzionale della ricerca

Seismic Station Installations and Their Impact on the Recorded Signals and Derived Quantities

This is the final peer-reviewed author's accepted manuscript (postprint) of the following publication:

*Published Version:*

castellaro s., alessandrini g., musinu g. (2022). Seismic Station Installations and Their Impact on the Recorded Signals and Derived Quantities. SEISMOLOGICAL RESEARCH LETTERS, 93(6), 3348-3362 [10.1785/0220220029].

*Availability:*

This version is available at: <https://hdl.handle.net/11585/904014> since: 2022-11-18

*Published:*

DOI: <http://doi.org/10.1785/0220220029>

*Terms of use:*

Some rights reserved. The terms and conditions for the reuse of this version of the manuscript are specified in the publishing policy. For all terms of use and more information see the publisher's website.

This item was downloaded from IRIS Università di Bologna (<https://cris.unibo.it/>).  
When citing, please refer to the published version.

(Article begins on next page)

This is the final peer-reviewed accepted manuscript of:

**Castellaro, S., G. Alessandrini, and G. Musinu (2022). Seismic Station Installations and Their Impact on the Recorded Signals and Derived Quantities, *Seismol. Res. Lett.* 93, 3348–3362**

The final published version is available online at <https://dx.doi.org/10.1785/0220220029>

Terms of use:

Some rights reserved. The terms and conditions for the reuse of this version of the manuscript are specified in the publishing policy. For all terms of use and more information see the publisher's website.

*This item was downloaded from IRIS Università di Bologna (<https://cris.unibo.it/>)*

***When citing, please refer to the published version.***

# Seismic Station Installations and their Impact on the Recorded Signals and Derived Quantities

Silvia Castellaro<sup>1\*</sup>, Giulia Alessandrini<sup>1</sup>, Giuseppe Musinu<sup>2</sup>

<sup>1</sup>Dipartimento di Fisica e Astronomia, Alma Mater Studiorum Università di Bologna, viale C. B. Pichat 8, 40127  
Bologna, Italy. \*Corresponding Author: [silvia.castellaro@unibo.it](mailto:silvia.castellaro@unibo.it)

<sup>2</sup>ENSER srl, viale A. Baccarini 29, Faenza, Ravenna – Italy

## Abstract

The role of local geology in controlling ground motion has long been acknowledged. Consequently, increasing attention is paid to the assessment of the geophysical properties of the soils at the seismic stations, which impact the station recordings and a series of related quantities, particularly those referring to seismic hazard estimates. Not the same level of attention is commonly dedicated to the seismic station installation, to the point that it is generally believed that housings/shelters containing seismic instruments are of no interest because they can only affect frequencies well above the engineering range of interest. By using examples from seismometric and accelerometric stations, we describe the 1) housing, 2) foundation and 3) pillar effects on the seismic records. We propose a simple working scheme to identify the existence of potential installation-related issues and to assess the frequency fidelity range of response of a seismic station to ground motion. Our scheme is developed mostly on ambient noise recordings and, thus, surface waves. The hope is that, besides the parameters (Vs30, soil classes etc.) that start to be routinely introduced in the seismic archives, the assessment of the maximum reliable frequency, under which no soil-structure interaction is expected, also becomes a mandatory information. In our experience, for some installation sites, the maximum reliable frequency can even be less than a very few Hz.

## Introduction

At the early stages of seismology, seismic stations were installed on stiff rock (Bormann, 2002), to minimize the effects of the fine sediments/rock weathering on the recorded seismic waves. The size of permanent installation seismometers, their need for screws, levelling, batteries and cables led to place them on artificial ground, such as *ad hoc* concrete slabs. There is also sometimes the improper perception that something stiff as a concrete slab or pillar between the sensor and the object of measurement improves the coupling between the two. In addition, to ensure protection from environmental conditions and vandalism, many seismic stations were placed inside small or large structures.

34 The need for homogenous and dense seismic networks and the increasing interest for the seismic site  
35 response and ‘local effects’ assessment, progressively required seismic stations to be installed on any type  
36 of geological condition. In parallel, growingg attention started to be paid to the characterization of the  
37 geophysical properties of the soils at the seismic stations (see Cultrera et al., 2021, for a review). In fact, their  
38 impact on the station recordings and on the subsequent hazard estimates can be large. On the opposite, not  
39 enough attention is still paid to the seismic station installation. It is generally recognized that this can affect  
40 the seismic recordings, but it is usually believed that housings/shelters can affect only frequencies well above  
41 the engineering range of interest. This led to the habit of naming ‘free-field stations’, stations that are not  
42 under free-field conditions (see also Hollender *et al.*, 2020, who noted the same issues).

43 The seismic sensor installation can affect seismometer recordings, both under microtremor and earthquake  
44 excitation, essentially in 3 strongly interconnected ways that we will discuss in the paper:

- 45 1) *Housing effect*: the structure/cabin inside which the sensor is installed has its own dynamics, ruled  
46 by its vibration modes. This motion is transmitted to the ground and recorded by the seismometer,  
47 even when the latter is placed on a pillar isolated from the foundation by means of a cut all around  
48 (Figure 1).
- 49 2) *Foundation effect*: stiff foundations (e.g., concrete slab on soft soils) perturb the incident wavefield.  
50 Typically, the horizontal motion recorded on the top of a foundation is strongly modified, compared  
51 to the free-field motion, at all the wavelengths smaller than and comparable to the foundation size.
- 52 3) *Pillar effect*: sensors are often placed on concrete pillars, detached from the foundation by means of  
53 a cut, with the intention of dynamically isolating the sensor from the surrounding  
54 foundation/structure. We will show that the proximity of the pillar to the foundation and the  
55 connection between the two provided by the ground, does not warrant the desired effect.

56 The effect of foundations on seismic motion was studied by several authors (e.g., Bycroft, 1980; Crouse and  
57 Husmand, 1989; Luco *et al.*, 1986; 1990; Castellaro and Mulargia, 2009; Hollender *et al.*, 2020; Cavalieri *et*  
58 *al.*, 2021). Luco *et al.* (1990), as an example, studied 12 different foundation geometries and performed a  
59 parametric study, by changing the size, the embedment depth, the extension above the surface. These  
60 results, however, strongly depended on the specific input used to study the phenomenon and the  
61 conclusions, though very relevant, were difficult to be used because they lacked generality.

62 As the result of an analysis conducted on earthquake recordings of 5 accelerometric French stations,  
63 Hollender et al. (2020) reported a general amplification at high-frequency (> 10 Hz).

64

65 On the opposite, focusing on surface waves, Bycroft (1978, 1980) recommended the use of large and thick  
66 foundations on nuclear power plants to reduce the seismic input to the overlying structures. If this reduction

67 is clearly welcome in the case of structures to protect them from seismic inputs, it is definitely unwelcome in  
68 the case of seismic stations, which are expected to faithfully record the incoming signal (at points 1 or 3 in  
69 Figure 1) and not its downsized version on the top of the foundation (point 2 in Figure 1).

70 The soil-structure interaction and the soil-city interaction were studied by even more authors (*Soil-structure:*  
71 Jennings, 1970; Wong and Trifunac, 1975; Bycroft, 1978; Safak, 1998; Guéguen *et al.*, 2000; Chavez-Garcia  
72 and Cardenas-Soto, 2002;; Mucciarelli *et al.*, 2003; Cornou *et al.*, 2004;; Guéguen and Bard, 2005;;  
73 Ditommaso *et al.*, 2010a,b; Laurenzano *et al.*, 2010; Massa *et al.*, 2010; Castellaro and Mulargia, 2011;  
74 Castellaro *et al.*, 2013;; Hollender *et al.*, 2020. *Soil-city:* Wirgin and Bard, 1996; Cloteau and Aubry, 2001;  
75 Guéguen *et al.*, 2002; Kham *et al.*, 2006; Schwan *et al.*, 2016; Isbilibroglu *et al.*, 2015; Kumar and Narayan,  
76 2018).

77 All these studies had little impact on the practical procedures behind seismic installations, also because their  
78 effect is hard to predict and to remove.

79 A recent trend is to move seismometers inside dedicated small fiber-glass cabins (e.g., CER panel in Figure  
80 2): the smaller the foundations, the smaller the range of wavelengths affected by the foundation itself. The  
81 smaller the protection structure, the larger its eigen-frequencies (thus beyond the frequency range of  
82 engineering interest). However, small fiber-glass structures have much lower stiffness  $k$  and mass  $m$   
83 compared to traditional structures and since the eigen-frequency of a structure is proportional to  $\sqrt{\frac{k}{m}}$ , these  
84 values can still fall inside the frequency range of engineering interest, altering the motion recorded by the  
85 seismometer.

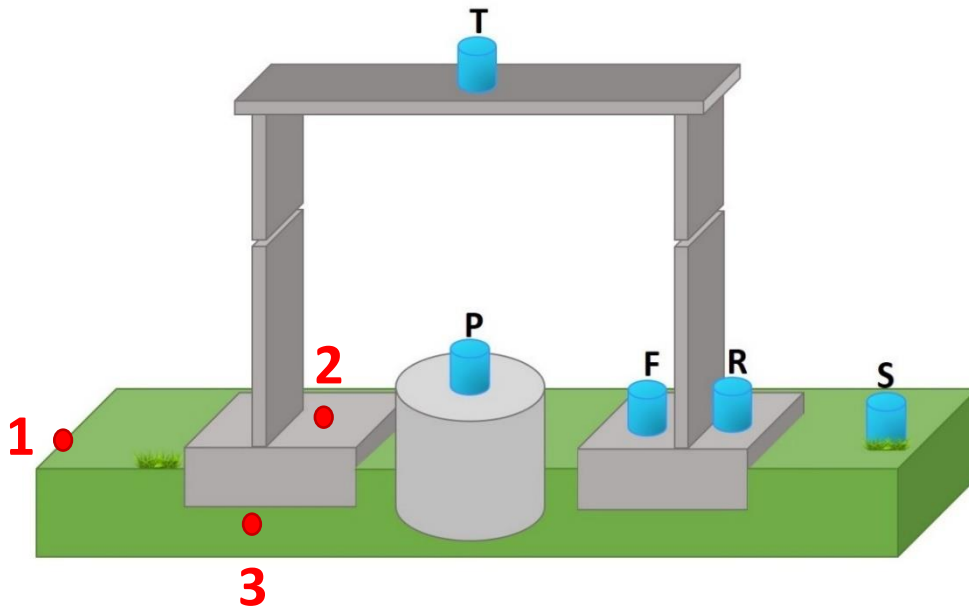
86 In this paper we provide some examples about: a) the elements that can affect the seismic station fidelity to  
87 ground motion, b) how to experimentally assess such fidelity.

88 Considering the variety of seismic installations that depends on national procedures, on specific soil  
89 conditions, on local construction habits, on seismic instrumentation and so on, we do not attempt any  
90 systematic/parametric study, but we illustrate the problems by using real examples from seismic stations  
91 belonging to the Italian National Seismic or Accelerometric (strong motion, IT) networks.

92 We use mostly ambient noise recordings, which are dominated by surface waves. Thus, we note since now  
93 that our conclusions can differ from those achieved numerically or experimentally by other authors (e.g.,  
94 Luco *et al.*, 1990; Hollender *et al.*, 2020) who used mostly earthquake recordings. However, as we are going  
95 to discuss, we all find that seismic records are severely altered by the soil-station interaction at mid-to-high  
96 frequencies.

97 We concentrate on ambient noise recordings because these types of data are increasingly used in passive  
98 seismic applications (seismic noise models, seismic site amplification assessments with ambient noise, etc.)  
99 and because ambient noise can be recorded continuously. This allows to obtain average values with narrow

100 standard deviation, which is often not the case when one can work only with few and very different  
101 earthquakes (in terms of size, depth, directivity, duration etc.).  
102 We focus on a few stations only, but the potential diffusion of the problem will be discussed at the end of  
103 the paper and, as noted by Hollender *et al.* (2020), it is not confined to single nations.



104  
105 *Figure 1. Schematic illustration of a typical seismic installation inside a small structure with a direct foundation. T (top) is the*  
106 *measurement point on the top of the structure (to characterize its fundamental mode), P on the pillar, F on the foundation, R on the*  
107 *foundation rim and S on natural soil.*

108

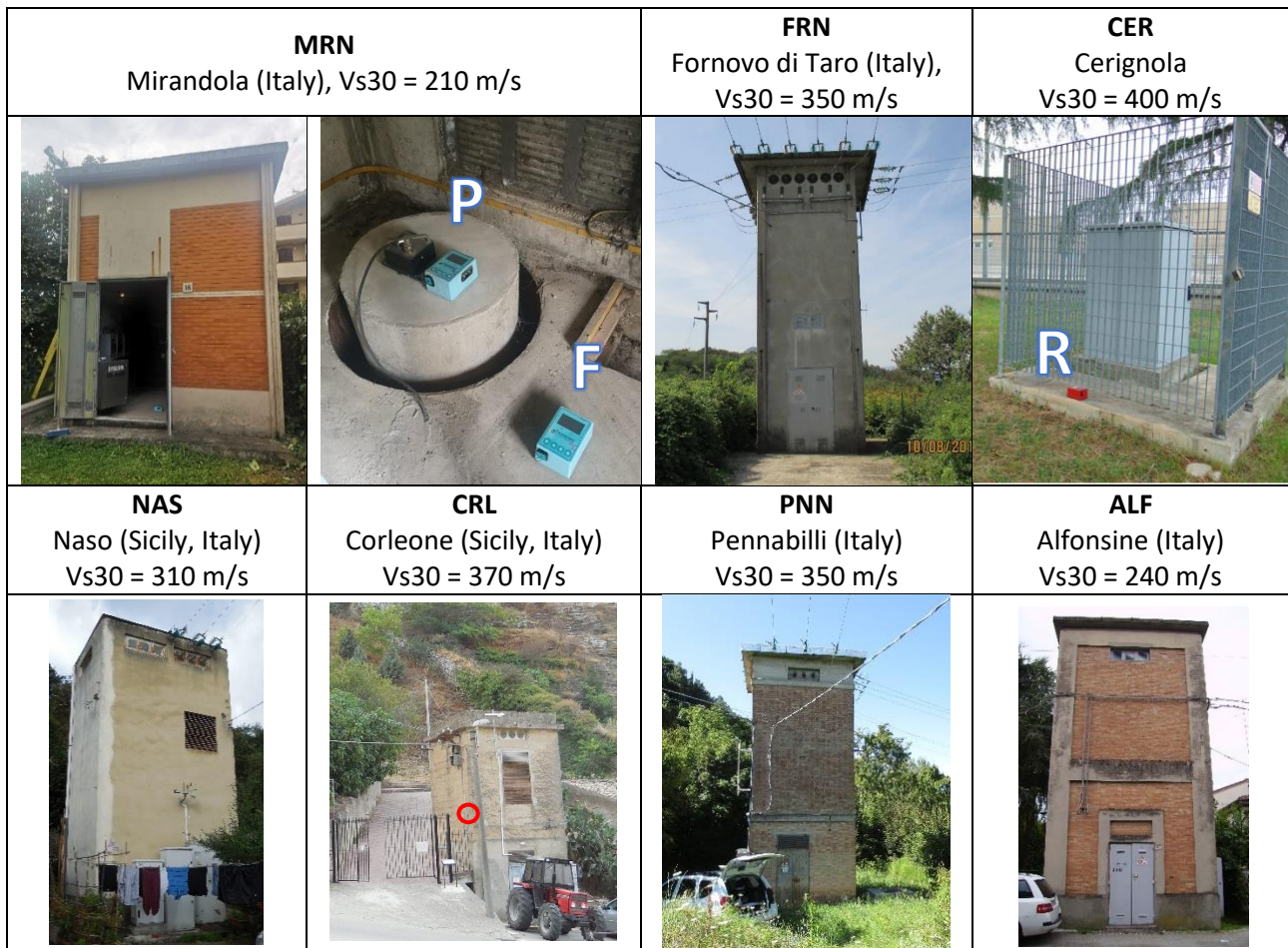
### 109 Elements that can affect the seismic station fidelity to ground motion

110 We refer to typical seismic stations settled inside big or small structures (Figure 1) and discuss the 1) housing,  
111 2) foundation and 3) pillar impact. These are strongly interconnected, therefore sometimes the discussion  
112 will necessarily mix them up.

113 We use examples from the Italian seismic/accelerometric stations illustrated in Figure 2. For each example  
114 we provide the station code, a picture and the soil type synthesized by means of its Vs30. Additional  
115 information about each station can be found by searching the station code in the INGV ItAcA database  
116 (D'Amico *et al.*, 2020). At the example sites, we collected simultaneous ambient noise measurements at the  
117 T (top), P (pillar), F (foundation), R (foundation rim), S (natural soil) locations given in Figure 1.

118 For all measurements we used Tromino® Blu 3-component portable velocity/acceleration sensors by MoHo  
119 srl (Italy), after checking that their response was identical. These instruments have a self-noise lower than  
120  $10^{-9} - 10^{-10}$  m/s at the frequencies of interest in this study ( $> 3$  Hz) and were set to have a resolution of  
121  $6 * 10^{-11}$  m/s in the  $\pm 0.5$  mm/s range. The signal was acquired at all sites for a minimum of 30 minutes,  
122 then split into non overlapping window. The FFT was applied to each window and the resulting spectra

123 were smoothed with triangular functions having a width equal to 3 per cent of the central frequency. In the  
 124 end, the average spectra and their standard deviations were computed.



125 *Figure 2. A set of stations of the Italian accelerometric (IT) and seismic (IV) network: small housing (MRN), tower-structures of the*  
 126 *national electric service (FRN, NAS, CRL, PNN, ALF) and fiber-glass cabin (CER). A typical pillar with the cut separating it from the*  
 127 *foundation is also shown for the MRN station. The pillar is present in most of the Italian installations and can also be square in shape,*  
 128 *as in the case of CER. The instruments used for this survey can be seen in the panel of MRN and CER (blue and red boxes). The letter P*  
 129 *stands for pillar, F for foundation, R for foundation rim.*

130

131 The housing effect

132

133 *Phenomenological evidence*

134 The influence of buildings on ground motion recorded by sensors inside or in their proximity is widely  
 135 acknowledged (see references in the Introduction). Less acknowledged is the direct influence of the housing  
 136 on the seismometer recordings that it should protect.

137 The motion of structures is ruled by the superposition of the motions occurring at their natural frequencies,  
 138  $f_{i=0, \dots, n}^{Stru}$ . When a structure vibrates – due to earthquakes, microtremor, wind – part of this vibration is  
 139 radiated to the soil and dissipated. The fraction of motion radiated back to the foundation can roughly be  
 140 estimated by measuring the spectral amplitude of motion on the top of the structure (T in Figure 1) and on

141 its foundation (F or R in Figure 1) or just off the foundation (S in Figure 1), at the same frequencies  $f_i^{Stru}$  and  
142 time. In practice, this fraction of motion is recorded also by the sensors placed on the pillar (P in Figure 1)  
143 because the vibration is efficiently transmitted through the ground.

144 To show this, we compare the spectra of the motion recorded on the top of the cabins with those recorded  
145 at the same time on the pillar or foundation (T/P and T/F ratios) and just outside the cabin (T/S ratios). We  
146 also compare the motion recorded on the pillar or foundation with the motion recorded in free-field (P/S,  
147 F/S ratios). When no effect is present, we expect these last two ratios to be equal to 1 at all frequencies.

148  
149 We start from the case of the MRN station, which is hosted in a small cabin (6pprox.. 4 m x 3 m x 4 m, Figure  
150 2), whose modal frequencies are 10 Hz (bending in the transversal direction) and 17 Hz (torsion, better visible  
151 in the measurement taken on the perimeter of the roof and clearly less in the proximity of the shear centre),  
152 as evident in the  $T/S_{ref}$  and  $T/F$  spectral ratios of Figure 3. We focus on the transversal direction because it is  
153 associated to the lowest resonance frequency, but the same discussion would apply to the longitudinal  
154 direction, along which the first bending mode is 15 Hz. We see that the  $F/S_{ref}$  and  $P/S_{ref}$  spectral ratios are  
155 identical, which means that the pillar sensor measures the same things as the foundation sensor, despite the  
156 cut all around it. This was observed also in Mucciarelli *et al.* (2003) and Castellaro and Mulargia (2009).

157 The  $F/S_{ref}$  ratio illustrates the role of the foundation on the incoming waves in respect to the real free-field  
158 condition. If the foundation had no effect, this ratio should be equal 1 at all frequencies, which is not.  $S_1/S_{ref}$   
159 is the ratio between the recording acquired on the soil just off the station ( $S_1$ ) and on the soil at a few meters  
160 distance from the station (usually less than 5 m,  $S_{ref}$ ). This ratio tends to 1 but there are still some minor  
161 differences due to the foundation still very close to  $S_1$ .

162 We note that if the pillar were isolated from the surrounding structure, we should not see any amplification  
163 in the  $P/S_{ref}$  spectra at the resonance frequencies of the structure. Figure 3 shows that this is not the case:  
164 the pillar is affected by the vibration modes of the overlying cabin, in the same way in which the foundation  
165 is ( $F/S_{ref}$ ).

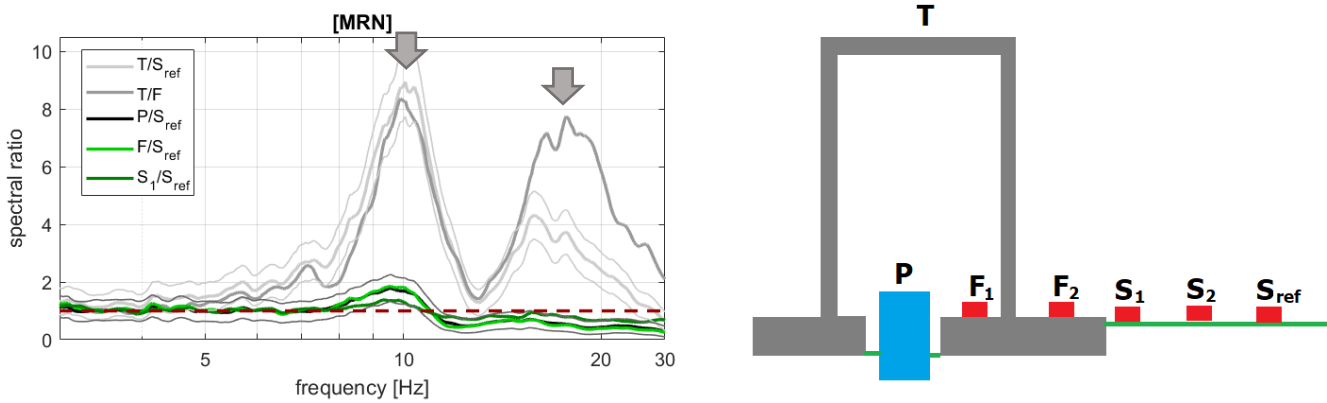
166 Despite the limited size of the hosting structure, we can assess, from the  $F/S_{ref}$  and  $P/S_{ref}$  ratios, that the  
167 motion recorded from this station is perturbed at frequencies larger than 8 Hz. The torsional mode (17 Hz) is  
168 not well acknowledgeable in the foundation measurements due to the foundation effect that we will discuss  
169 later in the text.

170 As a further example, we present in Figure 4 the spectral ratios recorded on the foundation vs. natural soil  
171 at two other larger-in-size stations (NAS and PNN, Figure 2). Again, we see that the seismic motion recorded  
172 at these sites is perturbed by the eigen-frequencies of the cabin at  $\approx 7$  Hz in one case and  $\approx 5$  Hz in the other



173 case. These are frequencies of large engineering interest, but the motion recorded from the seismometers  
 174 at these sites is not a faithful reproduction of the seismic input above  $\approx 6.5$  and 4 Hz, respectively.

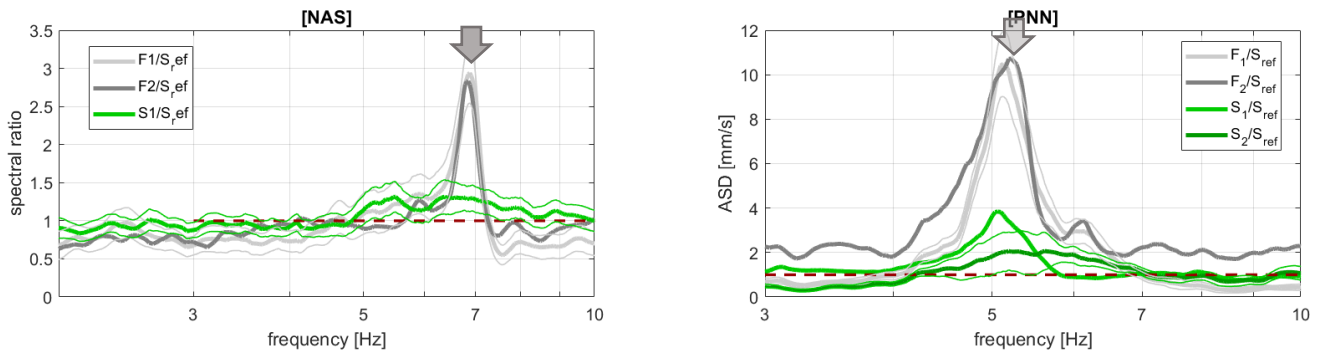
175



176

177 *Figure 3. Spectral ratios of the motion recorded along the transversal direction of the cabin MRN at different locations, whose symbols*  
 178 *are given in the right panel. The  $T/S_{ref}$  and  $T/F$  spectral ratios show the natural vibration modes of the structure (gray arrows at 10 Hz*  
 179 *mark the transversal bending mode, at 17 Hz a torsional mode). The  $P/S_{ref}$  and  $F/S_{ref}$  ratios show the effect of the foundation on the*  
 180 *incoming waves in respect to the real free-field condition. If the foundation induced no effect, these ratios should be equal 1 at all*  
 181 *frequencies.  $S_1/S_{ref}$  is the ratio between the recording acquired on the soil just off the station ( $S_1$ ) and on the soil at a few meters*  
 182 *distance from the station (usually 3-5 m from the foundation rim).  $S_1/S_{ref}$  tends to 1 but the eigen-mode of the structure is still visible.*  
 183 *The standard deviation of the spectral ratios is shown only in the two extreme cases, not to impair the readability of the plots. It was*  
 184 *checked that its amplitude is in the same order of magnitude also when not shown.*

185



186

187 *Figure 4. Spectral ratios of the motion recorded along the transversal direction of the cabins NAS and PNN at different locations,*  
 188 *whose symbols are given in the right panel of Figure 3. In the  $F/S_{ref}$  ratios the natural vibration modes of the structure (6.8 Hz and 5.2*  
 189 *Hz for NAS and PNN, respectively) can be clearly identified. These are progressively less noticeable in the  $S_1/S_{ref}$  and  $S_2/S_{ref}$  ratios. Thick*  
 190 *lines are the average values, thin lines indicate the standard deviations.*

191 *Effects on derived quantities*

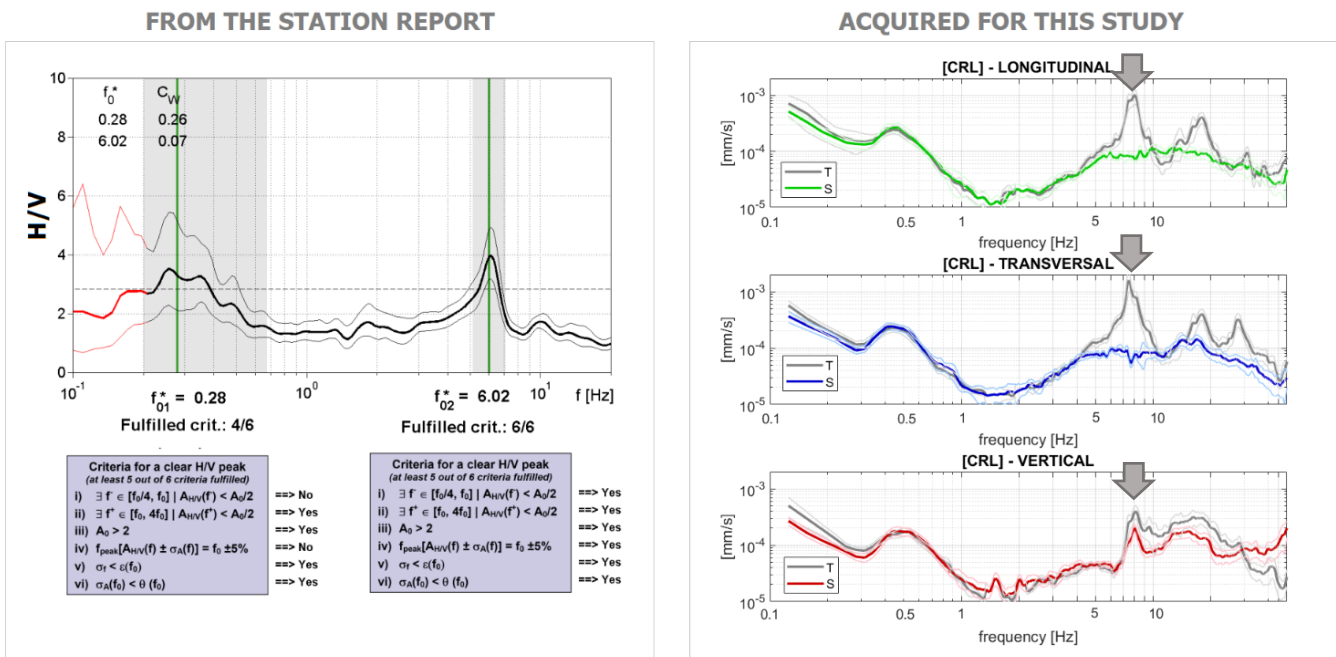
192 *On H/V*

193 Let us now consider the case of CRL station in Sicily (Figure 2). The H/V curve computed from the data  
 194 recorded by the official instrument installed on the pillar and provided by the national seismic agency is  
 195 shown on the left panel of Figure 5. It exhibits two peaks passing the SESAME (2004) criteria. In the official  
 196 station report, the 0.28 Hz frequency peak is indicated as fundamental mode of the site, while the 6 Hz  
 197 frequency peak is marked as an additional site frequency and it passes even more SESAME (2004) criteria  
 198 than the fundamental peak.

199 At this site we performed some measurements inside the niche in the wall of the cabin (red circle in Figure  
 200 1) and on the perimeter of the foundation, on natural soil. The spectra of these measurements (right panel  
 201 in Figure 5) clearly show that the natural modes of the cabin are 7, 18, 30 Hz and are not visible in the free-  
 202 field S recording, with the only exception of the small disturbance in the vertical component at the  
 203 fundamental frequency of the structure (7 Hz), which is an effect of structural rocking. This typically has an  
 204 amplitude which is 1/10 of the horizontal component amplitude.

205 The 6 Hz H/V peak frequency, identified in the official station report as ‘reliable’, is thus not a soil property  
 206 but the vibration mode of the cabin, as recorded by the pillar sensor. As a consequence, automatic peak  
 207 recognition algorithms in the case of sensors installed inside structures of any type should be avoided.

208 We take this opportunity to note that, despite its large use even on structures, the H/V method (here  
 209 providing a peak at 6 Hz) is not suitable to detect the resonance of structures (in this case 7 Hz). By dividing  
 210 the horizontal and vertical components, the H/V ratio mixes different structural behaviors, acting in different  
 211 directions and occurring at different frequencies. This easily result in a biased estimate of the structure  
 212 eigenfrequencies, as in this case.



213  
 214 *Figure 5. Left panel: H/V curve computed on the data acquired from the official instrument installed on the pillar at the CRL station.*  
 215 *According to the station report, 2 peaks pass the SESAME (2004) criteria. Our measurements (right panel), performed on the top of*  
 216 *the cabin (T) and on the natural soil just off the station (S) clearly show that the 6 Hz peak is the eigen-period of the cabin and not a*  
 217 *soil property. Thick lines are the average values, thin lines indicate the standard deviations.*

218  
 219 [On response spectra](#)

220 Let us now consider 10 intermediate size events (scaled to PGA = 0.25 g) recorded in real free-field conditions  
 221 (black curves in Figure 6) at the MRN site. We treat the MRN housing as single degree of freedom oscillator

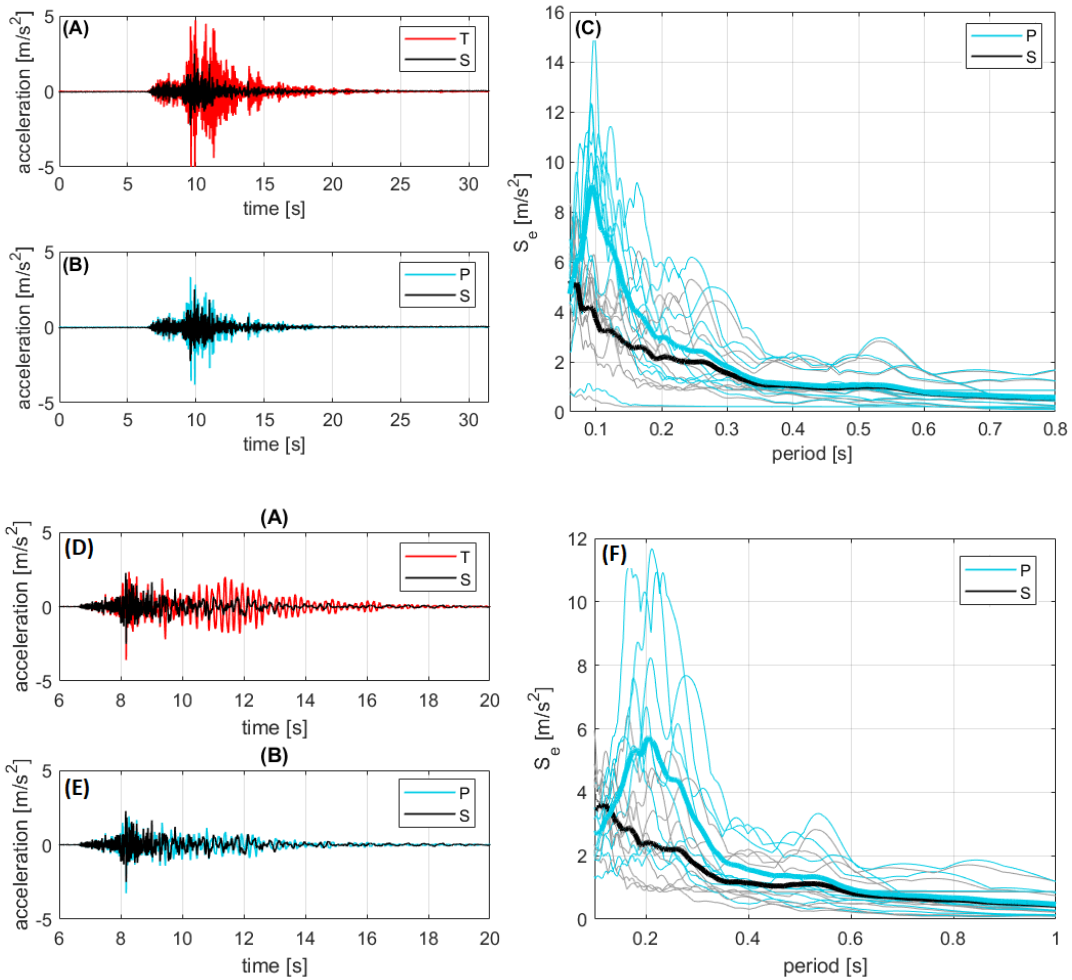
222 with natural frequency and damping as directly measured (10 Hz for the transversal component, Figure 3,  
223 and 5% damping as computed by the DECÒ method in Castellaro, 2016a). We ignore higher modes because  
224 they fall at frequencies of poor engineering interest. Alternatively, they could be considered by mode  
225 superposition. We compute the acceleration time series expected on the top of the cabin for the selected  
226 input earthquake (red curves in Figure 6a) by means of the Newmark integration approach (e.g., in Clough  
227 and Penzien, 1975).

228 From the T/P ratio in Figure 3 we know the fraction of the cabin motion transmitted to the pillar at all  
229 frequencies (e.g., 1/8 for the fundamental frequency), at least under ambient noise excitation. We can thus  
230 estimate the free-field motion that would be recorded by the seismometer on the pillar (cyan lines in Figure  
231 6b). This calculation might be not conservative, in the sense that under non-linear behavior it can  
232 underestimate the real impact.

233 We now compute the response spectra of the same input earthquakes as they would be computed from the  
234 pillar recording and from the free-field recording, and compare them in Figure 6c. The response spectra  
235 calculated from the signals collected on the pillar, P, are much larger than the response spectra computed  
236 from the free-field signals (S) at periods close to the natural periods of the housing.

237 In Figure 6d, e, f we show the same procedure applied to the FRN station (Figure 2). Since the FRN housing  
238 eigen-frequencies are lower than the MRN ones (5 Hz vs 10 Hz), the effect on the response spectrum is  
239 expected at larger periods, as it is in panel f.

240 Beyond the hypotheses and assumptions, these examples show that the response spectra computed from a  
241 recording performed on a pillar influenced by the surrounding structure can be severely affected at periods  
242 close to the structure eigen-period. PGA is also affected but to a minor extent (cyan, P, vs black, S, curves in  
243 Figure 6b, e).



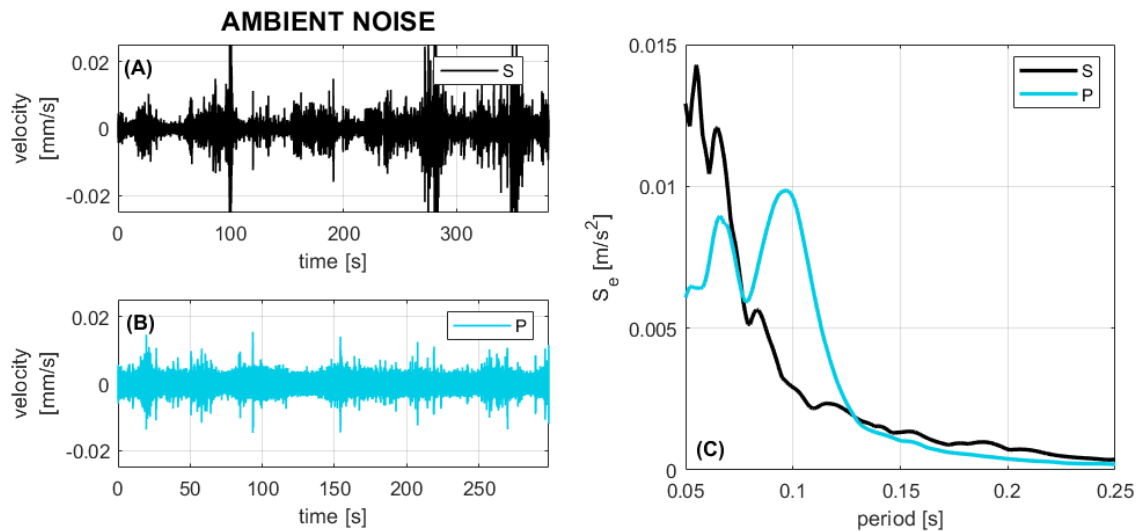
244

245

246 *Figure 6. Free-field earthquake records and response spectra ( $S$ , black) compared to those recorded on the top of a seismic station ( $T$ ,  
 247 red) and on the pillar inside the station ( $P$ , cyan). Panels a, b, c refers to the MRN station. Panels d, e, f to the FRN one. The average  
 248 response spectra (thick lines) are obtained from 10 earthquakes (thin lines). Panels a, b, d, e show just one of the 10 selected  
 249 earthquakes for each station, as an example.*

250

251 The results above come from models as no earthquake recordings were available on the top of the station,  
 252 on the pillar and on the surrounding real free-field conditions at the same time. However, to reproduce these  
 253 findings with real data, we used ambient noise recordings acquired simultaneously on the pillar and on the  
 254 garden surrounding the MRN station. The recordings lasted 30 minutes, to obtain a representative average  
 255 spectrum. As it can be seen in Figure 7, the response spectrum computed from the ambient noise recording  
 256 acquired on the pillar (cyan) shows the resonance modes of the cabin at 0.06 and 0.1 s (16 and 10 Hz) as  
 257 dominant peaks, while this is not the case for the response spectrum from ambient noise acquired on the  
 258 garden surrounding the structure. The two response spectra, in general, are very different.



259

260 *Figure 7. Ambient noise recording acquired in (A) free-field conditions, (B) on the station pillar and response spectra in the two cases*  
 261 *(C) for the MRN station. The input signal was 30 min long. Panel (A) an (B) show just a portion of it.*

262

## 263 The foundation effect

264

### 265 *General issues*

266 After the initial installations on rock, in more recent times seismic stations started to be installed on soft  
 267 sedimentary covers, both to improve the spatial coverage of seismic networks as well as to capture the so-  
 268 called seismic site effects (stratigraphic amplification, resonances, etc.). However, the standards of seismic  
 269 installations (concrete slabs or pillars inside the foundations of hosting structures), did not vary with the  
 270 underground geology and seismic stations keep on being installed following the original principles.

271 When an interface has to be placed between the object to measure and the measurement device, the  
 272 impedance between the interface and the object to measure must be as close as possible, to avoid  
 273 modifications of the signal due to the interface. This is well acknowledged in the down-hole and cross-hole  
 274 seismic testing, where, according to ASTM D7400/D7400M-19, the plastic hole casing must be coupled to the  
 275 ground by using a filling material with seismic impedance as close as possible to the ground itself. On the  
 276 opposite, this seems to be completely disregarded in seismic station installations. However, while a concrete  
 277 slab over stiff rocks is theoretically not expected to perturb seismic waves in a significant way, being the rock-  
 278 to-concrete transition virtually continuous, a concrete slab on soft sediments is expected to perturb seismic  
 279 waves significantly.

280 Foundations can be thought as stiff artificial layers that, when overlying softer ones, configure a 'velocity  
 281 inversion'. This effect on microtremors was largely discussed in Castellaro and Mulargia (2009). They showed  
 282 both empirically and analytically that whenever a stiffer layer overlies softer ones, the spectra recorded on  
 283 the stiff layer show deamplified horizontal components compared to the case with no velocity inversion. The

284 vertical component is generally less affected, to the point that a velocity inversion is typically marked by H/V  
285 ratios persistently lower than 1.

286 When a seismic wave hits a stiffer interface, the reflection coefficient is larger than the transmission  
287 coefficient (Zoeppritz, 1919). With reference to the red dots in Figure 1 it is generally expected that:

- 288 1) incoming surface waves hitting the foundation are reflected backwards and only a fraction of the  
289 incoming waves propagate through the medium, from point 1 to 3,
- 290 2) body waves travelling from the bottom to the surface are identically reflected downwards and only  
291 a fraction of the incoming wave propagates from point 2 to 3,
- 292 3) the foundation generates a velocity inversion, which inhibits the existence of the fundamental mode  
293 of Love waves (Castellaro, 2016b).

294 The waves affected by the aforementioned phenomena are, dominantly, those with wavelengths  $\lambda$   
295 comparable to or smaller than the twice the foundation dimensions (for example, a foundation of 5 m size  
296 on a clayey soil with  $V_s \approx 150$  m/s will affect approximately the frequencies  $f \geq 15$  Hz, see Figure 10). We  
297 warn, however, that the real effect is more complex, particularly in the case of earthquake input, as discussed  
298 in the Introduction (see also Luco *et al.*, 1990; Hollender *et al.*, 2020).

299 A decay in the horizontal spectra recorded on the foundation or pillar (F, R, P sites in Figure 1) compared to  
300 the real free-field conditions (site S in Figure 1) under microtremors is expected and effectively measured.  
301 This effect can easily be observed by taking two short measurements one on the foundation/pillar and one  
302 on the natural soil just around the foundation, as we are going to show.

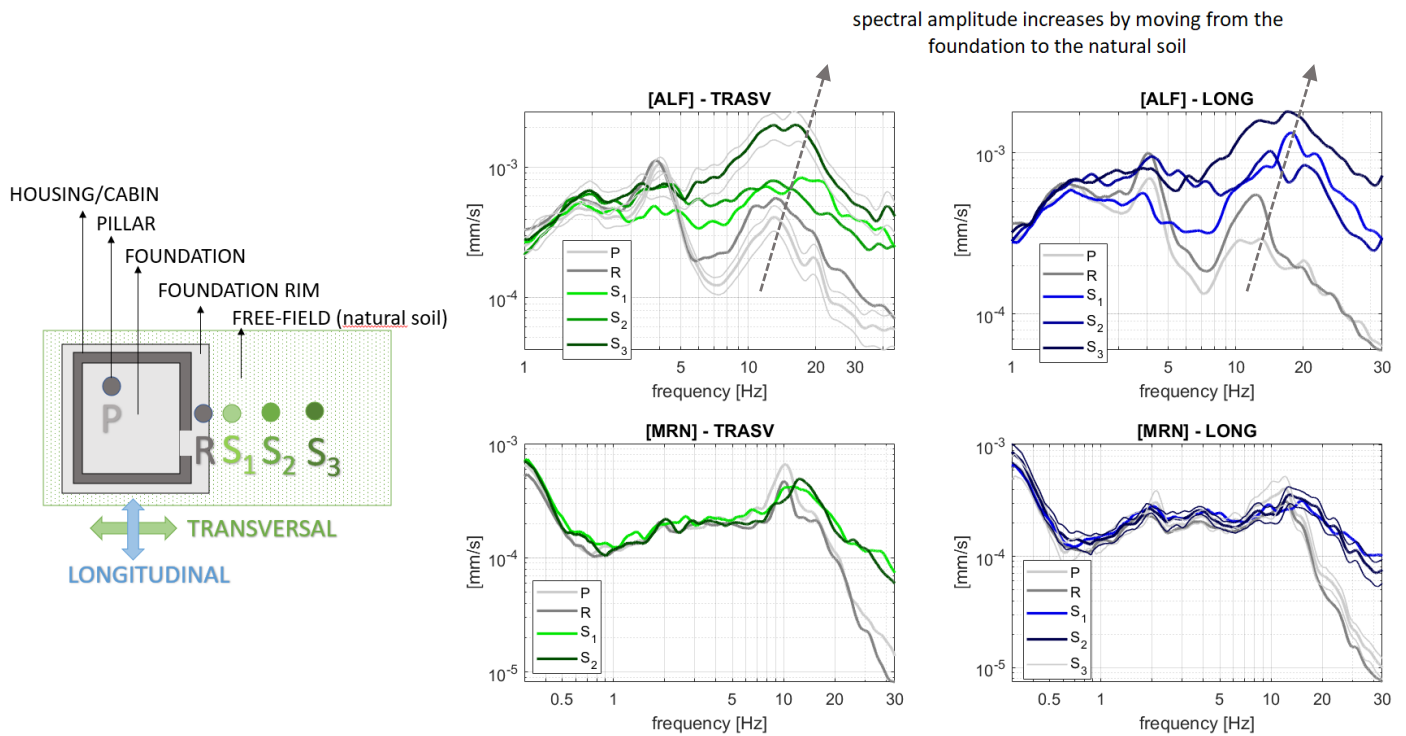
### 303 *Phenomenological evidence*

304 We consider the ALF and MRN seismic stations (Figure 1) and compare the spectra of the recordings taken  
305 on the pillar (P), on the foundation (F), on the foundation rim (R) and on the natural soil just outside the  
306 station (S), at the same time (Figure 8). We clearly see that while moving from the foundation center to its  
307 rim, to the natural soil, the amplitude of the horizontal spectra significantly increases. The effect is clear from  
308 4 Hz and 10 Hz upwards, for ALF and MRN respectively, and essentially depends on the foundation width,  
309 more than on its thickness (Castellaro and Mulargia, 2009). Again, there is no significant difference between  
310 the motion acquired on the pillars – just theoretically but not effectively isolated from the rest of the  
311 foundation – and the motion on the foundation. They both severely alter the recorded motion, compared to  
312 the soil one, of a factor up to 10 times in amplitude.

313 In Figure 8 (gray arrows) we clearly see that the F, P, R spectra are also severely affected by the natural  
314 frequencies of the housings (4 Hz for ALF and the already mentioned 10 Hz for MRN).

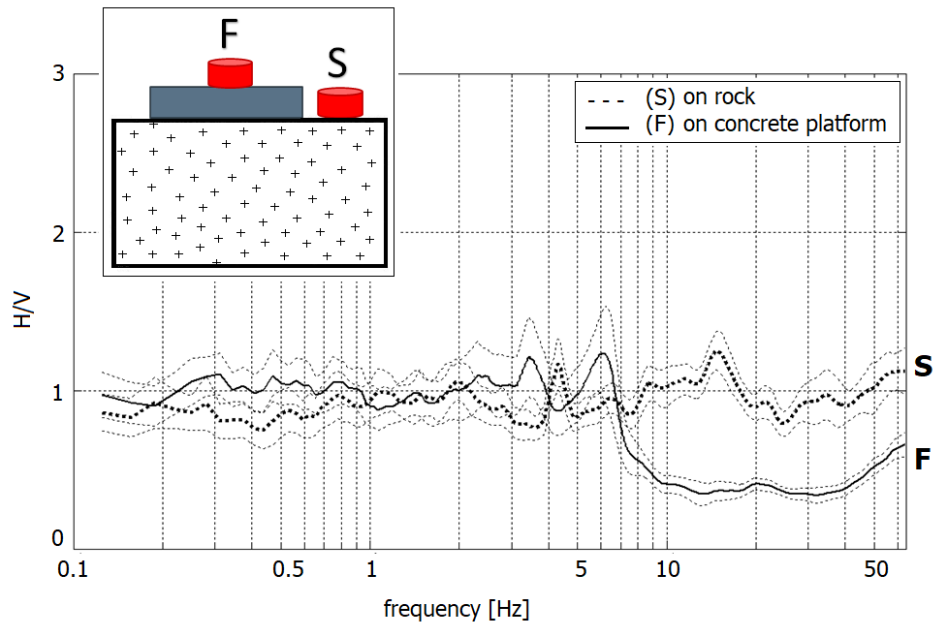
315 The foundation effect (decay in the horizontal spectral components) and the housing effect (peaks of  
 316 increased amplitude in the horizontal components at the eigen-frequencies of the housing) overlap and are  
 317 both present in the foundation (F) and pillar (P) recordings.

318 This issue is not typical only of foundations on soft soils. Outcropping rock is often weathered or detensioned,  
 319 as it occurs in tunnels, and this results in an impedance contrast between the rock and the foundation, too.  
 320 In Figure 9 we present the H/V curves acquired on a seismic station in Bulgaria (Sofia) installed inside a tunnel  
 321 in rock (granite). The acquisition performed on the rock shows a flat H/V with amplitude equal to 1, as  
 322 expected. The acquisition performed on the concrete platform constructed to host a number of instruments  
 323 on the rock, shows a significantly deamplified H/V ratio from 7 Hz upwards, due to the deamplification of the  
 324 horizontal components.



325  
 326 *Figure 8. Velocity spectra recorded at different sites at the ALF and MRN sites, by moving from the pillar to the foundation to the*  
 327 *surrounding soil. The typical distance between P and S3 is less than 10 m. Both the housing effect (peaks at 4 Hz for ALF, at 10 Hz for*  
 328 *MRN) and the foundation effect (deamplification of the horizontal components of motion at P and R compared to the soil sites S) are*  
 329 *visible. The standard deviation of the spectra is shown only in some extreme cases, not to impair the readability of the plots. Its*  
 330 *amplitude is approximately the same also when not shown.*

331



332

333 *Figure 9. Microtremor H/V ratio recorded on a granite rock (dashed line) and on a concrete slab on the rock (black line). The concrete*  
 334 *platform, being stiffer than the rock, produces a deamplified H/V curve at frequencies larger than 7 Hz.*

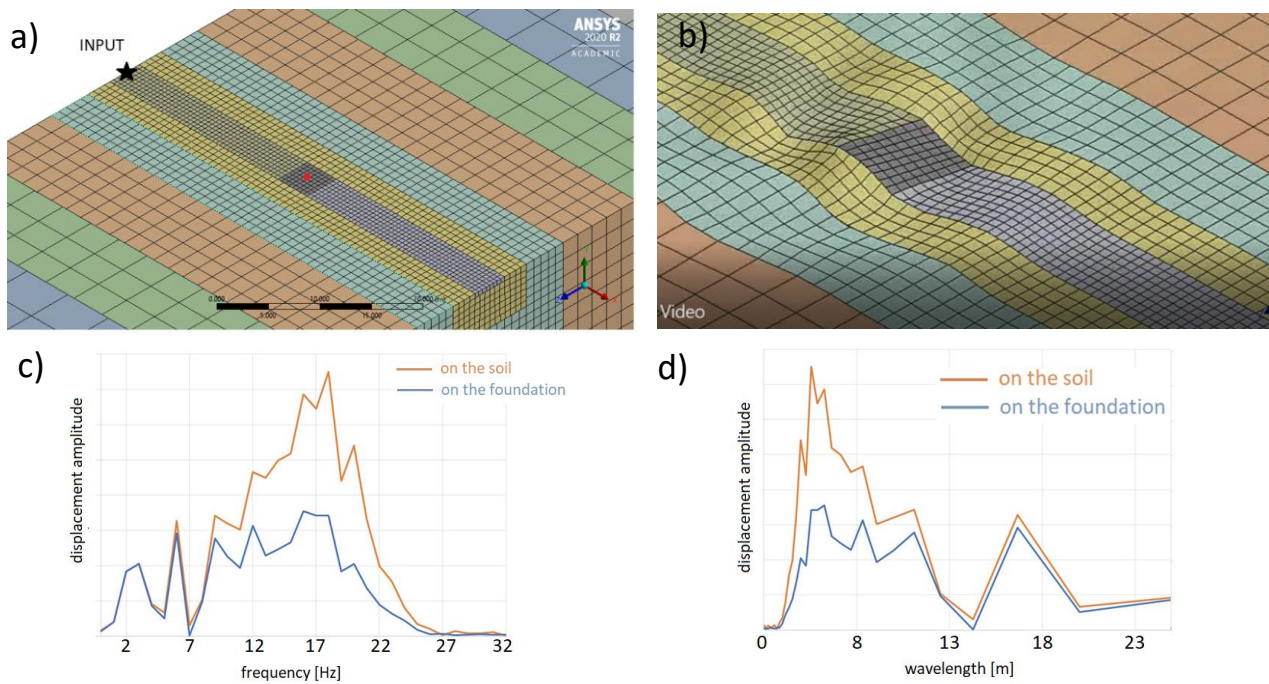
335

### 336 *Numerical evidence*

337 By using the FE numerical tools Ansys Academy 2020R1, we modelled a square concrete foundation slab ( $\rho$   
 338  $= 2400 \text{ kg/m}^3$ ,  $E = 30 \text{ GPa}$ , size  $4 * 4 \text{ m}^2$ ,  $0.5 \text{ m}$  thick) immersed in a soil ( $\rho = 2000 \text{ kg/m}^3$ ,  $\mu = 20 \text{ MPa}$ ;  $V_s = 100$   
 339  $\text{m/s}$ ). The mesh size was refined close to the slab, where we were interested in a better definition and was  
 340 coarser while moving away from the slab, to reduce the computation time. We input an impulsive motion  
 341 with horizontal direction on one side of the model (star in Figure 10a) that gives birth to surface waves  
 342 propagating and reaching the foundation slab, which is put into oscillation (Figure 10b). The reason for the  
 343 choice of an impulsive motion is that it is the ideal excitation, virtually containing the whole frequency  
 344 spectrum with the same amplitude (white noise).

345 The displacement amplitude spectrum recorded at the centre and on the top of the slab (red dot in Figure  
 346 10) is compared with the spectrum recorded at the same place but in the case of no foundation. A clear  
 347 deamplification of the motion on the slab can be seen from 20 Hz upwards (Figure 10c), which stands for a  
 348 deamplification at wavelengths lower than 10 m (which is twice the slab size, Figure 10d). This is what we  
 349 basically found experimentally with surface waves.





350 Figure 10. a) FE model of a slab (gray central square, 4\*4 m<sup>2</sup>) immersed in a soft soil. The different colors indicate the volumes with  
 351 meshes of different size. The underlying subsoil properties are uniform; b) the slab hit by surface waves generated by an input  
 352 applied at the star location of panel a); c) displacement spectra of the motion recorded at the centre and on the top of the slab and  
 353 the motion in case of no slab; d) as panel c) but in terms of wavelengths.

354

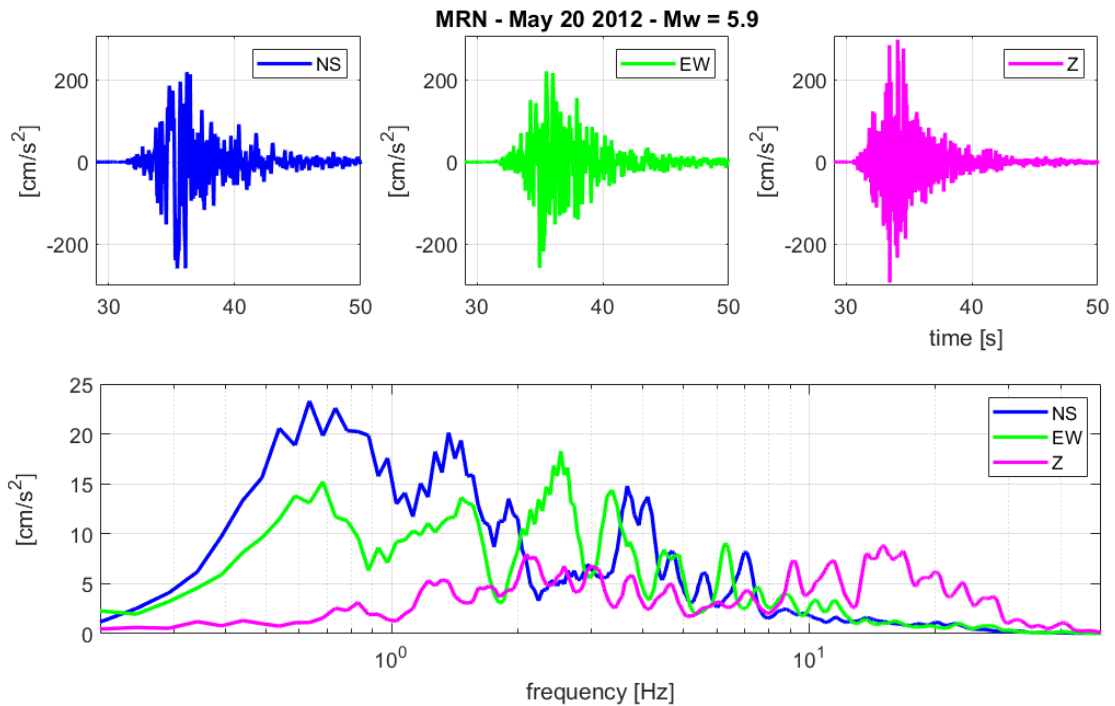
### 355 Other possible consequences

356 The deamplification of the horizontal components (H) due to a stiff foundation might sometime lead to the  
 357 wrong conclusion that the dominant component of motion during an earthquake is the vertical one (V). By  
 358 analyzing 123 response spectra of motion recorded at 41 alluvial sites, Bozorgnia *et al.* (1995) noted that the  
 359 H/V spectral ratios of motion were well below the assumed 1 to 2/3 value at frequencies larger than 6-10 Hz.  
 360 This is reported to be common in the near field (Chopra, 1966), but this could also be partly or fully explained  
 361 by the fact that near earthquakes are rich in high frequencies and that seismic installations – particularly  
 362 those settled on soft soils – modify the seismic input at high frequency, specifically decreasing its H/V ratio.

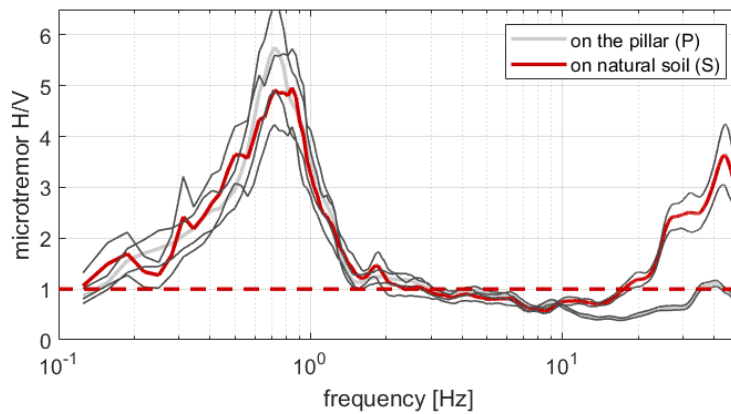
363 Luzi *et al.* (2013) observed that, during the May 20<sup>th</sup> 2012 Mw 5.9 earthquake, the closest-to-the-epicentre  
 364 MRN station recorded a vertical acceleration larger than the horizontal ones (Figure 11). A number of authors  
 365 mentioned this as one of the reasons for many of the observed collapses (Vannucchi *et al.*, 2012; Romeo,  
 366 2012; Ercolino *et al.*, 2012; Andreini *et al.*, 2014; Decanini *et al.*, 2012; Carydis *et al.*, 2012).  
 367 It is true that the Peak Ground Acceleration (PGA) recorded by the MRN station occurred in the vertical  
 368 component (Figure 11 top line), but the earthquake spectra (Figure 11 bottom line) show that the vertical  
 369 component was larger than the horizontal ones only at frequencies larger than  $\approx 10$  Hz.

370 This very same pattern (H/V < 1 at f > 10 Hz) is visible in the microtremor H/V spectra collected on the station  
 371 pillar but it is no more visible in the recordings collected at just 2 m distance from the station, in real free-  
 372 field conditions (Figure 12). We thus propose that in the case of this earthquake the dominant vertical

373 component of PGA was possibly not a real feature of the earthquake, but once more an artifact induced by  
 374 the foundation around the seismic sensor, that strongly deamplified the high frequency horizontal  
 375 components.



376  
 377 *Figure 11. 3C recordings of the Mirandola May 20<sup>th</sup> 2012 earthquake recorded at the MRN station. Top: time series. Bottom:*  
 378 *acceleration amplitude spectra.*



379  
 380 *Figure 12. Microtremor H/V ratios recorded at the MRN station on the pillar (P) and in free-field (S). The average value is marked by*  
 381 *the thick line, standard deviation is represented by the thin lines. The foundation effect is clear at frequencies larger than 10 Hz.*

382  
 383 **The pillar effect**

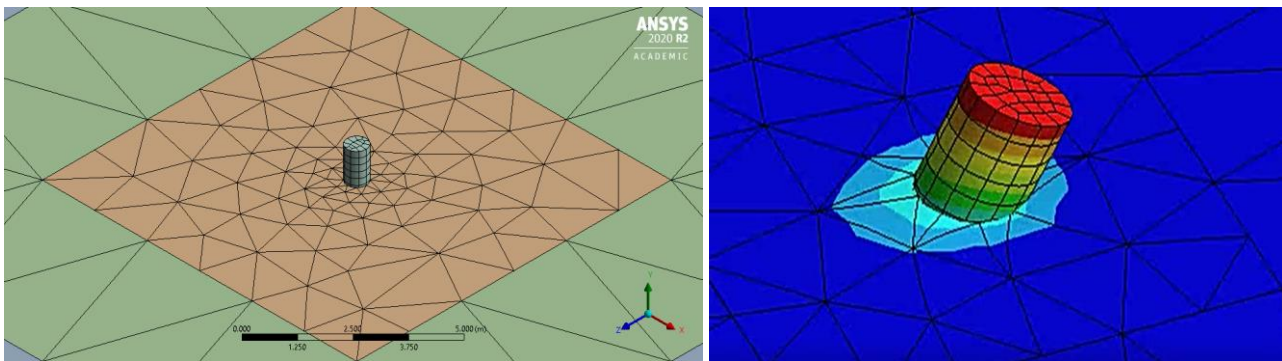
384 As anticipated, the intention of letting the seismometers be independent from the surrounding housings led  
 385 to the cut of the foundations and to the construction of pillars, directly set into the ground in the middle or  
 386 on the corner of foundations (Figure 1, MRN in Figure 2). Pillars are typically cylinders of 0.6 m diameter and  
 387 1.5 m height, set into the ground for at least 0.5 m. As seen, this cut is not much effective because the

388 structure and the pillar are rooted on the same soil and the transmission of the reciprocal motion is  
389 warranted by the soil itself.

390 Another potential problem emerges. Also pillars have their own vibration modes that are certainly recorded  
391 by the sensor applied on their top. Do these modes occur at frequencies of engineering interest? Concrete  
392 pillars typically installed in seismic stations are 'beams' dominated by shear, rather than flexural deformation  
393 and their eigen-modes are expected to occur at several tens of hertz, well beyond the range of interest in  
394 engineering seismology.

395 The eigen-frequency of a shear beam with a fixed constraint can be computed analytically. However, in the  
396 presence of an earthquake excitation the soil should be considered as an elastic body and a numerical  
397 investigation is more suitable. By using again the FE numerical tools Ansys Academy 2020R1, we modelled a  
398 pillar with the dimensions given above, density  $\rho = 2.4 \cdot 10^3 \text{ kg/m}^3$ , Young modulus  $E = 30 \text{ GPa}$ , stuck for  
399 0.5 m into a soil with  $\rho = 2 \cdot 10^3 \text{ kg/m}^3$ ,  $E = 45 \text{ MPa}$ ,  $V_S = 150 \text{ m/s}$  (Figure 13). By applying an impulse  
400 in horizontal direction with  $V_0 = 1 \text{ m/s}$  and observing the free oscillations, we found that the eigen-  
401 frequency of the pillar is 28 Hz. This is hard to measure in real cases because the pillars are thick and the  
402 displacement under microtremor very weak, however we can expect that on average this kind of pillars  
403 vibrates at frequencies around 30 Hz and this value increases if, e.g., they are stuck at shallower depth.

404 It can be expected that the pillar moves independently from the foundation during an earthquake. However,  
405 the reduction in the horizontal components due to the foundation effect on surface waves still exist, as well  
406 as the transmission of the housing eigen-modes through the soil, as we have shown in the previous examples.



407  
408 *Figure 13. FE model of a homogenous pillar stuck into a soft soil.*

409

#### 410 Diffusion and identification of the problem

411 We estimated that as of 2021, in Italy, at least 35% of the  $\approx 600$  accelerometric IT stations are hosted inside  
412 4-5 m side, 7-9 m height towers of the electrical national service (Figure 14). A further 3% are hosted in other  
413 types of buildings and 18% inside minihouses, that is structures like the MRN case we discussed. Most of  
414 them is also settled on soft soils (C, D, E categories according to EC8), where soil-structure interaction is  
415 expected to be large. We thus expect that the aforementioned issues affect at least half of the accelerometric

416 IT Italian network (clearly with different severity according to the specific conditions), but this is certainly not  
417 an issue restricted to Italy (see also Hollender *et al.*, 2020).

418 We propose a simple way to identify the existence of a potential installation-induced problem and assess the  
419 range of fidelity of the response of a seismic station to the ground motion. The approach is based on the  
420 following actions:

- 421 1) take a recording on the top of the seismic cabin (T) to identify its natural frequency,
- 422 2) take a set of simultaneous recordings on the pillar (P), on the foundation (F) and under truly free-  
423 field conditions (S). We are aware that at some sites a ‘truly free-field’ condition cannot even be  
424 achieved. We also warn that ‘simultaneous’ here means just at the same time but with no need for  
425 a real synchronization of all instruments, as no phase but only amplitude spectra are analyzed,
- 426 3) compare T and P (or T and F) spectra: these will immediately reveal the degree of rocking of the  
427 housing and tell what fraction of the housing motion is radiated to the foundation under weak  
428 motion,
- 429 4) compute the F/S or P/S spectral ratios. This will reveal to what extent the sensors placed on the  
430 foundation/pillar record a deamplified horizontal motion compared to the real free-field conditions  
431 and in what frequency interval. Expect that the larger the foundation size, and the softer the soil  
432 compared to the foundation, the larger the frequency interval affected by these issues.

433 We warn that the recordings to assess the structure eigen-frequencies (item 1) should be done along the  
434 structural main axes, but these may not coincide with the NS-EW axes of the seismometer/accelerometer  
435 installed inside the structure. In this case, *ad hoc* axis rotations should be performed.  
436 We also warn that in order to perform the comparisons above, some spectral smoothing is mandatory but  
437 this should not exceed a few percent of the central frequency otherwise the spectral peaks due to the housing  
438 eigenmodes will appear less clear.

439 The proposed approach is based on our experience with ambient noise recordings. The seismic installation  
440 impact during earthquake motion can be different and is certainly more difficult to be predicted because it  
441 depends on a number of additional factors (earthquake directivity, depth, size etc.).

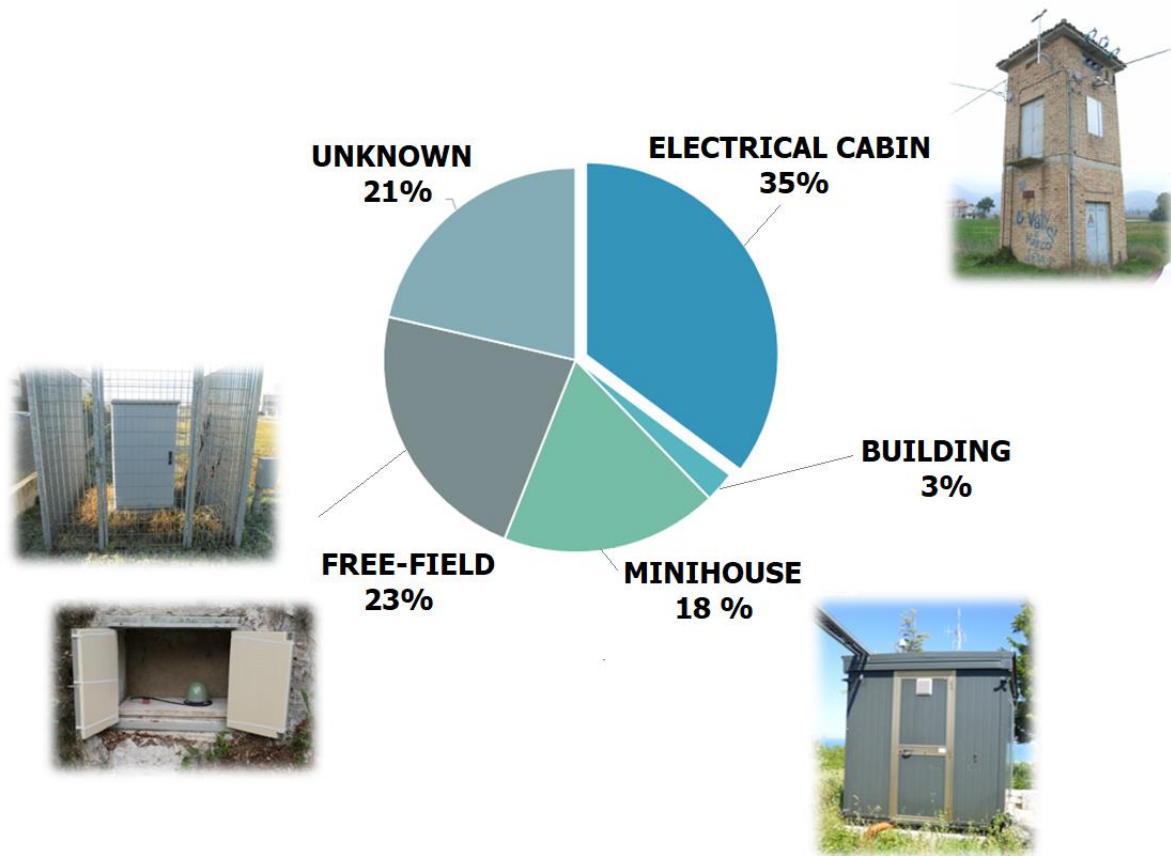


Figure 14. Percentage of the seismic installations of the Italian accelerometric network, as of 2021.

442

443

444

#### 445 Discussion and Conclusions

446 Bormann *et al.* (2002, chapter 7) wrote that seismic site selection is not often given the amount of study it  
 447 requires. Maybe also the hosting structure is not given the consideration it requires (Hollender *et al.*, 2020)  
 448 as the design and construction of seismic stations has not much evolved over time.

449 The presence of a structure around an instrument perturbs the recorded motion in a way that can be  
 450 summarized in three effects.

451 The first one is the transmission of the structure own motion to the foundation and the surrounding ground.  
 452 Sensors placed inside the structure record, therefore, a composite signal, made of seismic waves and of the  
 453 response of the structure to them. We showed that cutting the foundation around the sensor pillars gives no  
 454 benefits in isolating the sensor from the housing motion, as the vibrations are transmitted very efficiently  
 455 through the common soil.

456 The second effect is that a foundation, typically made of reinforced concrete, acts as a layer with seismic  
 457 impedance much higher than any natural soil. Surface waves striking an extended rigid layer like a  
 458 foundation, will be mostly reflected backwards as they hit the foundation. They will shake the structure, but  
 459 only a small fraction of them will cross the foundation and will be recorded by the instruments installed on

460 the foundation. Foundations violate the principle of physical measurements according to which when an  
461 interface is needed between an instrument and the object of measurement (the ground) then the interface  
462 must have an impedance as close as possible to the object of measurement, to minimize the perturbation of  
463 the wavefield. Concrete slabs/pillars do not have this property, not even always when installed on very stiff  
464 rock.

465 As a consequence, in seismic tremor recordings carried out inside a structure, a fraction of waves is missing.  
466 The numerical and experimental evidence on earthquake data is not so clear in terms of deamplification.  
467 Luco *et al.* (1990) and Hollender *et al.* (2020) documented more often the opposite effect, that is of  
468 amplification at frequencies larger than 10 Hz. However, in both cases (ambient noise and earthquakes) the  
469 seismic motion is strongly altered by the presence of the foundation.  
470 The third issue is related to the pillar that can alter the recorded motion by means of its own eigenmodes.  
471 This effect, however, is mostly confined to frequencies beyond the range of engineering interest.

472 We noted that particularly the first problem can affect even the modern fibre-glass installations since their  
473 smaller mass and stiffness combination turns into natural frequencies of vibration still falling within the range  
474 of engineering interest. Fiber-glass cabins are also often hosted on large concrete slabs where other  
475 instruments (typically meteorological) are installed. This makes the frequency interval, where  
476 deamplification of horizontal motion recorded by the seismometer is measured, wider.

477 Installing seismic stations inside structures does not affect the earthquake magnitude estimates, that are  
478 usually performed at very long periods and does not affect the hypocentral estimates, which are based on  
479 the arrival times of specific waves.

480 However, even by excluding the installations inside proper buildings, the soil-structure interaction at the  
481 seismic stations placed on surface can, in our experience, produce artefactual patterns at least down to 2 Hz,  
482 (this depends on the size and properties of the housing). The influence of the cabin self-modes on the  
483 recordings also leads to artefactual spikes in the response spectra typically on the plateau. The opposite (a  
484 reduction in the response spectra) effect is expected because of the velocity inversion induced by the  
485 foundation.

486 Besides the fact that these two effects can partly compensate in the response spectra, an issue remains about  
487 the reliability of the motion recorded from the seismic stations at high frequency. The strong-  
488 motion/accelerometric sensors and the short-period seismometers, which are dedicated to the detection of  
489 the mid-to-high-frequency motion, are thus those most affected by the seismic installation. This has  
490 consequences in the assessment of the station H/V curves, of seismic site effects in terms of PGA, on the  
491 computation of attenuation laws and ground motion prediction equations but probably also on the often  
492 observed unexpected large vertical motion compared to the horizontal one during earthquakes.

493 In conclusion, we believe that besides the parameters ( $V_{s30}$ , soil classes etc.) that start to be routinely  
494 introduced in the seismic archives, assessing the maximum reliable frequency  $f_{max}$  of earthquake and  
495 microtremor recordings (under which no soil-structure interaction is expected) is a mandatory step. To this  
496 aim, it should also be reminded that due to the possible non-elastic behavior under strong motion, such  $f_{max}$   
497 established under weak motion could even be overestimated. This is because the eigen-frequencies of  
498 structures under strong-motion can be lower than under ambient noise excitation again due to the soil-  
499 structure interaction. We provided a simple scheme to assess this maximum reliable frequency  $f_{max}$ .

500 As a very final ‘detail’, we observe that seismometer/accelerometers also have natural frequencies, meant  
501 as resonances of the instrumental case. Accelerometers are usually smaller and screwed to the pillars, which  
502 makes the natural frequencies of their boxes (and content) shift to very large values. On the opposite, when  
503 dealing with bulky long-period seismometers, the natural frequency of their case (and content) can be in the  
504 range of few tens of hertz. This also depends on the instrument-to-soil/pillar/foundation coupling. In some  
505 extreme cases, particularly with temporary installations, also this point could be considered because it can  
506 lead to artefactual amplification of the recorded motion above 10 Hz.

507

## 508 [Data and Resources](#)

509 The data collected at the seismic station installations were collected by the authors and by those mentioned  
510 in the acknowledgments. The accelerometric records used in this paper were provided by ITACA (D’Amico *et*  
511 *al.*, 2020), [INGV Itaca](#), last accessed Jan. 2022.

512

## 513 [Declaration of Competing Interests](#)

514 The authors acknowledge there are no conflicts of interest recorded.

515

## 516 [Acknowledgments](#)

517 We thank Giovanni Lattanzi for Figure 1, Martina Delvecchio and Anna Ferrara for the computations used to  
518 build Figure 14, Antonella Gorini from Dipartimento della Protezione Civile for providing access to the MRN  
519 station and the two workers from ENEL who assisted us during the measurements. We thank Stefano Isani  
520 for the continuous support in terms of structure dynamics. We thank Alfredo Pitullo and the Consorzio per  
521 la Bonifica della Capitanata (Contratto di Consulenza Commissionata tra Consorzio per la Bonifica della  
522 Capitanata e Dipartimento di Fisica e Astronomia dell’Alma Mater Studiorum – Università di Bologna 2019-  
523 2021) for funding some of the presented surveys. We thank Umberto Borgia, Luigi Perricone and Riccardo  
524 Panzeri for their help, in 2014, in collecting many of the measurements here presented, in the frame of the

525 DPC-INGV-S2-2014 Project “Constraining Observations into Seismic Hazard”, which is here acknowledged,  
526 too. Long time has passed since then, but the memory of those days is still alive. Thank you.

527

## 528 [References](#)

529 Andreini, M., A. De Falco, L. Giresini L., M. Sassu (2014). Structural damage in the cities of Reggiolo and Carpi  
530 after the earthquake on May 2012 in Emilia Romagna, *Bull. Earthquake Eng.* **12** 2445-2480.

531 Bormann, P. (2012). New Manual of Seismological Observatory Practice (NMSOP-2), Potsdam: Deutsches  
532 GeoForschungszentrum GFZ, IASPEI.

533 Bozorgnia, Y., M. Niazi, K.W. Cambell (1995). Characteristics of Free-Field Vertical Ground Motion during the  
534 Northridge Earthquake, *Earth. Spectra* **11** 515-525.

535 Bycroft, G.N. (1978). Soil-structure interaction at higher frequency factors, *Earthq. Eng. Struct. Dyn.* **5** 235-  
536 248.

537 Bycroft, G.N. (1980). Soil-foundation interaction and differential ground motions, *Earthq. Eng. Struct. Dyn.* **8**  
538 235-248.

539 Castellaro, S. (2016a). Soil and structure damping from single station measurements, *Soil Dyn. Earthq. Eng.*  
540 **90** 480-493.

541 Castellaro, S. (2016b). The complementarity of H/V and dispersion curves, *Gephysics* **81** T323-T338.

542 Castellaro, S., F. Mulargia (2009). The effect of velocity inversions on H/V, *Pure and Applied Geophysics* **166**  
543 567-592.

544 Castellaro, S., F. Mulargia (2010). How far from a building starts the tremor free-field? The case of three most  
545 famous Italian towers and of a modern building, *Bull. Seism. Soc. Am.* **100** 2080-2094.

546 Castellaro, S., L.A. Padron, F. Mulargia (2013). The different response of apparently identical structures: a far-  
547 filed lesson from the Mirandola 20<sup>th</sup> May 2012 earthquake, *Bull. Earthq. Eng.*, **12**, 2481-2493.

548 Cavalieri, F., A.A. Correia, R. Pinho, (2021). Variations between foundation-level recordings and free-field  
549 earthquake ground motions: numerical study at soft-soil sites, *Soil Dynamics and Earthquake*  
550 *Engineering* **141** 106511.

551 Carydis, P., C. Castiglioni, E. Lekkas, I. Kostaki, N. Lebesis, A. Drei (2012). The Emilia Romagna, May 2012  
552 earthquake sequence. The influence of the vertical earthquake component and related geoscientific and  
553 engineering aspects, *Ingegneria Sismica* **2-3**, 31-58.

554 Chavez-Garcia, F.J., M. Cardenas-Soto (2002). The contribution of the built environment to the free-field  
555 ground motion in Mexico City, *Soil Dyn. Earthq. Eng.* **22** 773–780.

556 Chopra, A.K. (1966). The importance of the vertical component of earthquake motions, *Bull. Seism. Soc. Am.*  
557 **56** 1163-1175.

558 Clough, R.W., J. Penzien (1975). *Dynamics of structures*, Mc-Graw Hill.



559 Clouteau, D., D. Aubry (2001). Modifications of the ground motion in dense urban areas, *J. Computational*  
560 *Acoustics* **9** 1659-1675.

561 Cornou, C., P. Guéguen, P.-Y. Bard, E. Haghshenas (2004). Ambient noise energy bursts observation and  
562 modeling: Trapping of harmonic structure-soil induced-waves in a topmost sedimentary layer, *J.*  
563 *Seismol.* **8** 507–524.

564 Crouse, C.B., B. Husmand (1989). Soil-structure interaction at CDMG and USGS accelerograph stations, *Bull.*  
565 *Seismol. Soc. Am.* **79** 1–14.

566 Cultrera, G., C. Cornou, G. Di Giulio, P.-Y. Bard (2021). Indicators for site characterization at seismic station:  
567 recommendation from a dedicated survey, *Bull. Earthquake Eng.* **19** 4171–4195

568 D'Amico, M.C., C. Felicetta, E. Russo, S. Sgobba, G. Lanzano, F. Pacor, L. Luzi (2020). ITalian ACcelerometric  
569 Archive (ITACA), version 3.1, Istituto Nazionale di Geofisica e Vulcanologia (INGV).

570 Decanini, L.D., D. Liberatore, L. Liberatore, L. Sorrentino (2012). Preliminary Report on the 2012, May 20,  
571 Emilia Earthquake, v.1, <http://www.eqclearinghouse.org/2012-05-20-italy-it/>

572 Ditommaso, R., M.R. Gallipoli, M. Mucciarelli, F.C. Ponzio (2010a). Effect of a single vibrating building on free-  
573 field ground motion: numerical and experimental evidences, *Bulletin of Earthquake Engineering* **8** DOI:  
574 10.1007/s10518-009-9134-5.

575 Ditommaso, R., S. Parolai, M. Mucciarelli, S. Eggert, M. Sobiesiak, J. Zschau (2010b). Monitoring the response  
576 and the back-radiated energy of a building subjected to ambient vibration and impulsive action: the  
577 Falkenhof Tower (Potsdam, Germany), *Bulletin of Earthquake Engineering* **8** DOI: 10.1007/s10518-009-  
578 9151-4.

579 Ercolino, M., G- Magliulio, G. Manfredi (2016). *The lesson learnt after Emilia-Romagna earthquakes on*  
580 *precast RC structures: a case-study*, 1st International Conference on Natural Hazards & Infrastructure  
581 28-30 June, Chania, Greece.

582 Guéguen, P., P.-Y. Bard, C.S. Oliveira (2000). Experimental and numerical analysis of soil motion caused by  
583 free vibration of a building model, *Bull. Seism. Soc. Am.* **90** 1464-1479.

584 Guéguen, P., P.-Y. Bard, F.J. Chavez-Garcia (2002). Site-city seismic interaction in Mexico Citylike  
585 environments: An analytic study, *Bull. Seism. Soc. Am.* **92** 794- 811.

586 Guéguen, P., P.-Y. Bard (2005). Soil-structure and soil-structure-soil interaction: experimental evidence at the  
587 Volvi test site, *J. Earthq. Eng.*, **9**, 657–693.

588 Hollender, F., Z. Roumelioti, E. Maufroy, P. Traversa, A. Mariscal (2020). Can we trust high-frequency content  
589 in strong-motion database signals? Impact of housing, coupling, and installation depth of seismic  
590 sensors, *Seismological Research Letters* **91** 2192-2205.

591 Isbilibiroglu, Y., R. Taborda, J. Bielak, (2015). Coupled Soil-Structure Interaction Effects of Building Clusters  
592 during Earthquakes, *Earthq. Spectra* **31** 463-500.

593 Jennings, P.C. (1970). Distant motion from a building vibration test, *Bull. Seism. Soc. Am.* **60** 2037-2043.

594 Kham, M., J.-F. Semblat, P.-Y. Bard, P. Dangla. (2006). Seismic site–city interaction: main governing  
595 phenomena through simplified numerical models, *Bull. Seism. Soc. Am.* **96** 1934-1951.

596 Kumar N., J.P. Narayan, 2018. Quantification of site–city interaction effects on the response of structure  
597 under double resonance condition, *Geophysical Journal International* **212** 422–441.

598 Laurenzano, G., E. Priolo, M.R. Gallipoli, M. Mucciarelli, F.C. Ponzio (2010). Effect of vibrating buildings on  
599 free-field motion and on adjacent structures: the Bonefro (Italy) case history, *Bull. Seism. Soc. Am.* **100**  
600 802-818.

601 Luco, J.E., J.G. Anderson, M. Georgevich (1990). Soil-structure interaction effects on strong motion  
602 accelerograms recorded on instrument shelters, *Earthq. Eng. Struct. Dyn.* **19** 119-131.

603 Luco, J., H.L. Wong (1986). Response of a rigid foundation to a spatially random ground motion, *Earthq. Eng.*  
604 *Struct. Dyn.* **14** 891-908.

605 Luzi, L., F. Pacor, G. Ameri, R. Puglia, P. Burrato, M. Massa, P. Augliera, G. Franceschina, S. Lovati, R. Castro  
606 (2013). Overview on the Strong-Motion Data Recorded during the May–June 2012 Emilia Seismic  
607 Sequence, *Seismological Research Letters*, **84** 629-644.

608 Massa, M., S. Marzorati, C. Ladina, S. Lovati (2010). Urban seismic stations: soil-structure interaction  
609 assessment by spectral ratio analyses, *Bull. Earthquake Eng.* **8** 723–738.

610 Mucciarelli, M., M.R. Gallipoli, F.C. Ponzio, M. Dolce (2003). Seismic waves generated by oscillating building,  
611 *Soil Dyn. Earthq. Eng.* **23** 255-262.

612 Romeo, R. (2012). Emilia (Italy) M5.9 earthquake on 20 May 2012: an unusual pattern of liquefaction, *Italian*  
613 *J. Eng. Geol. Environ.* **2** 75-84.

614 Şafak, E. (1998), New approach to analyzing soil-building systems, *Soil Dyn.and Earthq. Engin.* **17** 509-517.

615 Schwan, L., C. Boutin, L.A. Padron, M.S. Dietz, P.-Y. Bard, C. Taylor (2016). Seismology Site-city interaction:  
616 theoretical, numerical and experimental crossed-analysis, *Geophys. J. Int.* **205** 1006–1031.

617 SESAME (2004). Guidelines for the implementation of the H/V spectral ratio technique on ambient vibrations:  
618 Measurements, processing and interpretation, SESAME European Research Project WP12, deliverable  
619 no. D23.12.

620 Vannucchi, G., T. Crespellani, J. Facciorusso, A. Ghinelli, C. Madiati, A. Puliti, S. Renzi (2012). Soil liquefaction  
621 phenomena observed in recent seismic events in Emilia-Romagna Region, Italy, *Ingegneria Sismica* **2-3**  
622 20-29.

623 Wirgin, A., P.-Y. Bard (1996). Effects of building on the duration and amplitude of ground motion in Mexico  
624 City, *Bull. Seism. Soc. Am.* **86** 914-920.

625 Wong, H.L., M.D. Trifunac (1975). Two dimensional antiplane building-soil-building interaction for two or  
626 more buildings and for incident plane SH waves, *Bull. Seismol. Soc. Am.* **65** 1863-1865.

627 Zoeppfritz, K. (1919). On reflection and propagation of seismic waves, *Gottinger Nachrichten* **1** 66-84.

628

- 629 Silvia Castellaro - Dipartimento di Fisica e Astronomia, Alma Mater Studiorum Università di Bologna, viale C. B. Pichat  
630 8, 40127 Bologna Italy, [silvia.castellaro@unibo.it](mailto:silvia.castellaro@unibo.it)
- 631 Giulia Alessandrini - Dipartimento di Fisica e Astronomia, Alma Mater Studiorum Università di Bologna, viale C. B.  
632 Pichat 8, 40127 Bologna Italy, [giulia.alessandrin11@unibo.it](mailto:giulia.alessandrin11@unibo.it)
- 633 Giuseppe Musinu - ENSER srl, viale A. Baccharini 29, 48018 Faenza, Ravenna – Italy, [giuseppe.musinu@enser.it](mailto:giuseppe.musinu@enser.it)
- 634

635 List of figure captions

636

637 **Figure 1.** Schematic illustration of a typical seismic installation inside a small structure with a direct  
638 foundation. T (top) is the measurement point on the top of the structure (to characterize its fundamental  
639 mode), P on the pillar, F on the foundation, R on the foundation rim and S on natural soil.

640 **Figure 2.** A set of stations of the Italian accelerometric (IT) and seismic (IV) network: small housing (MRN),  
641 tower-structures of the national electric service (FRN, NAS, CRL, PNN, ALF) and fiber-glass cabin (CER). A  
642 typical pillar with the cut separating it from the foundation is also shown for the MRN station. The pillar is  
643 present in most of the Italian installations and can also be square in shape, as in the case of CER. The  
644 instruments used for this survey can be seen in the panel of MRN and CER (blue and red boxes). The letter P  
645 stands for pillar, F for foundation, R for foundation rim.

646 **Figure 3.** Spectral ratios of the motion recorded along the transversal direction of the cabin MRN at different  
647 locations, whose symbols are given in the right panel. The  $T/S_{ref}$  and  $T/F$  spectral ratios show the natural  
648 vibration modes of the structure (gray arrows at 10 Hz, 17 Hz). The  $P/S_{ref}$  and  $F/S_{ref}$  ratios show the effect of  
649 the foundation on the incoming waves in respect to the real free-field condition. If the foundation induced  
650 no effect, these ratios should be equal 1 at all frequencies.  $S_1/S_{ref}$  is the ratio between the recording acquired  
651 on the soil just off the station ( $S_1$ ) and on the soil at a few meters distance from the station (usually 3-5 m  
652 from the foundation rim).  $S_1/S_{ref}$  tends to 1 but the eigen-mode of the structure is still visible. The standard  
653 deviation of the spectral ratios is shown only in the two extreme cases, not to impair the readability of the  
654 plots. It was checked that its amplitude is in the same order of magnitude also when not shown.

655 **Figure 4.** Spectral ratios of the motion recorded along the transversal direction of the cabins NAS and PNN  
656 at different locations, whose symbols are given in the right panel of Figure 3. In the  $F/S_{ref}$  ratios the natural  
657 vibration modes of the structure (6.8 Hz and 5.2 Hz for NAS and PNN, respectively) can be clearly identified.  
658 These are progressively less noticeable in the  $S_1/S_{ref}$  and  $S_2/S_{ref}$  ratios. Thick lines are the average values, thin  
659 lines indicate the standard deviations.

660 **Figure 5.** Left panel: H/V curve computed on the data acquired from the official instrument installed on the  
661 pillar at the CRL station. According to the station report, 2 peaks pass the SESAME (2004) criteria. Our  
662 measurements (right panel), performed on the top of the cabin (T) and on the natural soil just off the station  
663 (S) clearly show that the 6 Hz peak is the eigen-period of the cabin and not a soil property. Thick lines are the  
664 average values, thin lines indicate the standard deviations.

665 **Figure 6.** Free-field earthquake records and response spectra (S, black) compared to those recorded on the  
666 top of a seismic station (T, red) and on the pillar inside the station (P, cyan). Panels a, b, c refers to the MRN  
667 station. Panels d, e, f to the FRN one. The average response spectra (thick lines) are obtained from 10  
668 earthquakes (thin lines). Panels a, b, d, e show just one of the 10 selected earthquakes for each station, as  
669 an example.

670 **Figure 7.** Ambient noise recording acquired in (A) free-field conditions, (B) on the station pillar and response  
671 spectra in the two cases (C) for the MRN station. The input signal was 30 min long. Panel (A) and (B) show just  
672 a portion of it.

673 **Figure 8.** Velocity spectra recorded at different sites at the ALF and MRN sites, by moving from the pillar to  
674 the foundation to the surrounding soil. The typical distance between P and S3 is less than 10 m. Both the  
675 housing effect (peaks at 4 Hz for ALF, at 10 Hz for MRN) and the foundation effect (deamplification of the  
676 horizontal components of motion at P and R compared to the soil sites S) are visible. The standard deviation  
677 of the spectra is shown only in some extreme cases, not to impair the readability of the plots. Its amplitude  
678 is approximately the same also when not shown.

679 **Figure 9.** Microtremor H/V ratio recorded on a granite rock (dashed line) and on a concrete slab on the rock  
680 (black line). The concrete platform, being stiffer than the rock, produces a deamplified H/V curve at  
681 frequencies larger than 7 Hz.

682 **Figure 15.** a) FE model of a slab (gray central square, 4\*4 m<sup>2</sup>) immersed in a soft soil. The different colors  
683 indicate the volumes with meshes of different size. The underlying subsoil properties are uniform; b) the slab  
684 hit by surface waves generated by an input applied at the star location of panel a); c) displacement spectra  
685 of the motion recorded at the centre and on the top of the slab and the motion in case of no slab; d) as panel  
686 c) but in terms of wavelengths.

687 **Figure 11.** 3C recordings of the Mirandola May 20<sup>th</sup> 2012 earthquake recorded at the MRN station. Top: time  
688 series. Bottom: acceleration amplitude spectra.

689 *Figure 12.* Microtremor H/V ratios recorded at the MRN station on the pillar (P) and in free-field (S). The  
690 average value is marked by the thick line, standard deviation is represented by the thin lines. The foundation  
691 effect is clear at frequencies larger than 10 Hz.

692 **Figure 13.** FE model of a homogenous pillar stuck into a soft soil.

693 **Figure 14.** Percentage of the seismic installations of the Italian accelerometric network, as of 2021.

694

695

696

697